










# Repolarization indicates electrical instability in ventricular arrhythmia originating from papillary muscle

Paula Münkler <sup>1,2\*</sup>, Niklas Klatt<sup>1</sup>, Katharina Scherschel <sup>1,2,3,4</sup>,  
Pawel Kuklik <sup>1,5</sup>, Christiane Jungen <sup>1,2,6</sup>, Ersin Cavus <sup>1</sup>, Christian Eickholt<sup>1,5</sup>,  
Jan Christoph<sup>7</sup>, Marc D. Lemoine<sup>1,2</sup>, Torsten Christ <sup>2,8</sup>, Stephan Willems<sup>1,2,5</sup>,  
René Riedel <sup>1,9,10</sup>, Paulus Kirchhof<sup>1,2,11</sup>, and Christian Meyer<sup>1,2,3,4</sup>

<sup>1</sup>Department of Cardiology, University Heart and Vascular Center Hamburg, University Hospital Hamburg-Eppendorf, Martinistraße 52, 20246 Hamburg, Germany; <sup>2</sup>DZHK (German Centre for Cardiovascular Research), Partner Site Hamburg/Kiel/Lübeck, Berlin, Germany; <sup>3</sup>Division of Cardiology, Angiology and Intensive Care, Cardiac Neuro- and Electrophysiology Research Consortium (cNEP), EKV Düsseldorf, Düsseldorf, Germany; <sup>4</sup>Cardiac Neuro- and Electrophysiology Research Consortium (cNEP), Medical Faculty, Heinrich Heine University Düsseldorf, Kirchfeldstraße 40, 40217, Düsseldorf, Germany; <sup>5</sup>Department of Cardiology, Asklepios Hospital St Georg, Lohmühlenstraße 5, 20099, Hamburg, Germany; <sup>6</sup>Department of Cardiology, Leiden University Medical Center, Leiden, The Netherlands; <sup>7</sup>Cardiovascular Research Institute University of California, San Francisco, 555 Mission Bay Blvd South, 352S, San Francisco, CA, USA; <sup>8</sup>Institute of Experimental Pharmacology and Toxicology, University Medical Centre, Martinistraße 52, 20246 Hamburg, Germany; <sup>9</sup>Max Planck Institute for Evolutionary Biology, Plön, Germany; <sup>10</sup>German Rheumatism Research Centre Berlin—an Institute of the Leibniz Association, Berlin, Germany; and <sup>11</sup>Institute of Cardiovascular Sciences, University of Birmingham, Birmingham, UK

Received 18 December 2021; accepted after revision 30 June 2022; online publish-ahead-of-print 22 August 2022

## Aims

Cardiac arrhythmia originating from the papillary muscle (PM) can trigger ventricular fibrillation (VF) and cause sudden cardiac death even in the absence of structural heart disease. Most premature ventricular contractions, however, are benign and hitherto difficult to distinguish from a potentially fatal arrhythmia. Altered repolarization characteristics are associated with electrical instability, but electrophysiological changes which precede degeneration into VF are still not fully understood.

## Methods and results

Ventricular arrhythmia (VA) was induced by aconitine injection into PMs of healthy sheep. To investigate mechanisms of degeneration of stable VA into VF in structurally healthy hearts, endocardial high-density and epicardial mapping was performed during sinus rhythm (SR) and VA. The electrical restitution curve, modelling the relation of diastolic interval and activation recovery interval (a surrogate parameter for action potential duration), is steeper in VA than in non-arrhythmia (ventricular pacing and SR). Steeper restitution curves reflect electrical instability and propensity to degenerate into VF. Importantly, we find the parameter repolarization time in relation to cycle length (RT/CL) to differentiate self-limiting from degenerating arrhythmia with high specificity and sensitivity.

## Conclusion

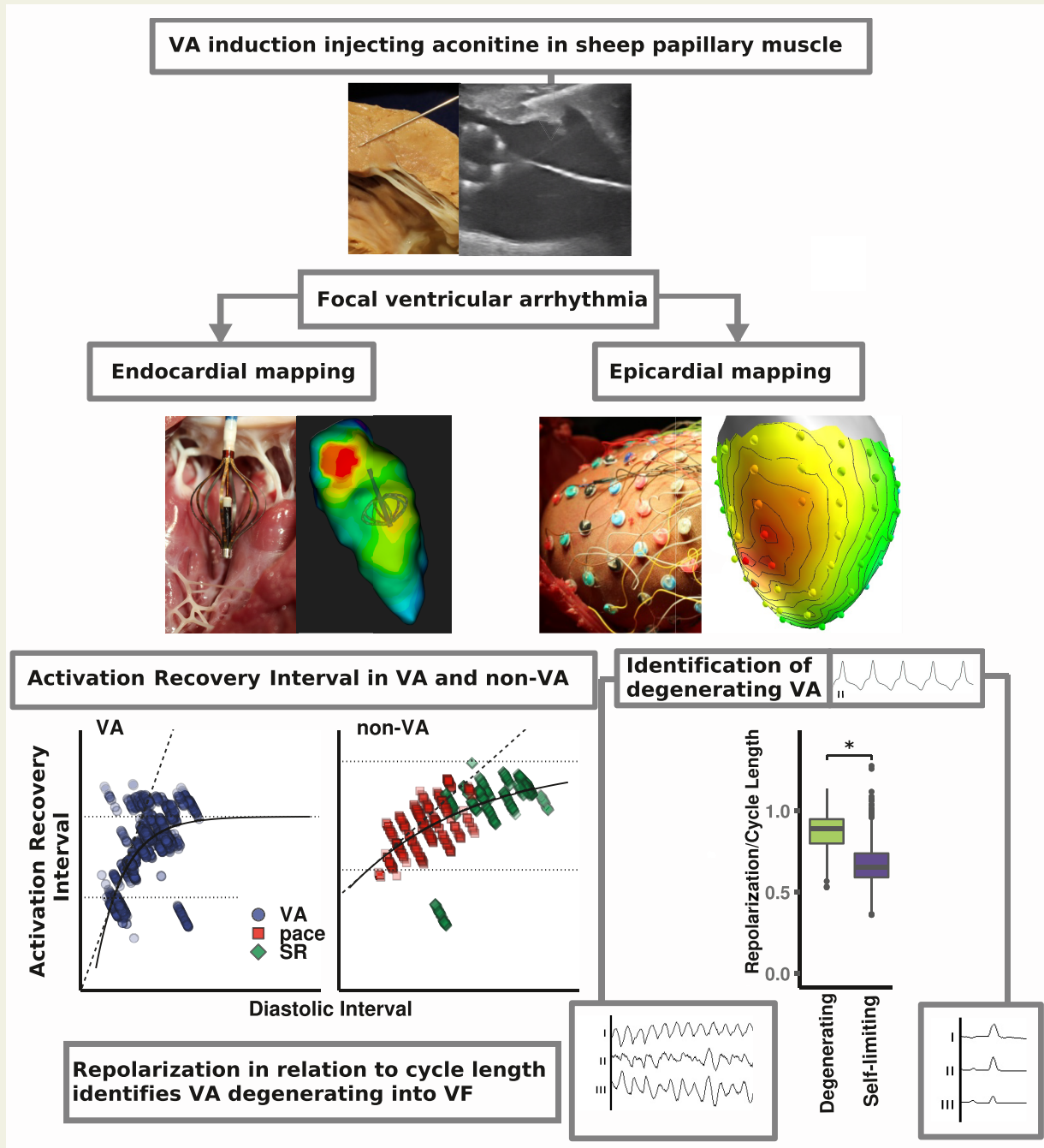
RT/CL may serve as a simple index to aid differentiation between self-limiting and electrically unstable arrhythmia with the propensity to degenerate to VF. RT/CL is independent of cycle length and could easily be measured to identify electrical instability in patients.

\* Corresponding author. Tel: +49 040 7410 0; fax: +49 040 7410 55862. E-mail address: p.muenkler@uke.de

© The Author(s) 2022. Published by Oxford University Press on behalf of the European Society of Cardiology.

This is an Open Access article distributed under the terms of the Creative Commons Attribution-NonCommercial License (<https://creativecommons.org/licenses/by-nc/4.0/>), which permits non-commercial re-use, distribution, and reproduction in any medium, provided the original work is properly cited. For commercial re-use, please contact [journals.permissions@oup.com](mailto:journals.permissions@oup.com)

Graphical Abstract



Keywords

Ventricular arrhythmia • Sudden cardiac death • Electrical instability • Animal model • Repolarization

Introduction

Sudden cardiac death, next to suicides and traffic accidents, is one of the three most common causes of death in young adults.<sup>1</sup> Detecting the risk for sudden death remains difficult, especially in patients

without clinical signs of a cardiac condition and with preserved left ventricular function.<sup>2</sup> As demonstrated in seminal work by Haissaguerre and colleagues, ventricular arrhythmia (VA) arising from Purkinje fibres can be a trigger of ventricular fibrillation (VF) and thereby cause sudden cardiac death in patients without

## What's new

- The site of origin of aconitine-induced ventricular arrhythmia (VA) is indicated by a custom-made epicardial electrode sock and high-resolution endocardial mapping.
- The electrical restitution curve is steeper in VA compared with sinus rhythm and pacing, identifying electrically unstable arrhythmia.
- Repolarization time in relation to cycle length identifies degenerating VA distinguishing them from stable and self-limiting VA.

detectable structural heart disease.<sup>3–5</sup> Papillary muscles (PMs) in particular show a dense network of Purkinje fibres, implying arrhythmogenic potential of this anatomical structure. Ventricular arrhythmia originating from the PM is indeed a possible trigger of VF.<sup>6,7</sup> Hence, for the present study, the PM was selected as an injection site for aconitine.

It is known that disturbed repolarization is associated with the electrical instability and occurrence of VA, e.g. after myocardial infarction.<sup>8</sup> Whether repolarization kinetics do contribute to lethal VA originating from the PM remains unclear. Therefore, the clinical availability of a simple marker allowing the risk stratification and identification of potentially lethal VA would have a substantial value in patient care.

The activation recovery interval (ARI) is a surrogate for action potential duration.<sup>9</sup> The duration of action potentials is modulated by changes in the preceding diastolic interval (DI).<sup>10,11</sup> The relationship between DI and the subsequent ARI is known as electrical restitution kinetics: relatively short DI provoking a more pronounced decrease in the subsequent ARI reflects electrical instability as a steep restitution curve (ARI~DI).<sup>12–15</sup> Electrical instability is represented by a steeper electrical restitution curve and is considered to reflect predisposition for the degeneration of regular heart rhythm into VF.<sup>16</sup> Hitherto, no functional parameters have been established which allow the identification of arrhythmic sites during electroanatomical mapping in electrophysiological procedures in routine clinical settings.

Here we characterize repolarization kinetics, including electrical restitution curves,<sup>17,18</sup> in a model of VA in sheep provoked by aconitine injection<sup>19</sup> directly into PM to quantify the impact of repolarization to degeneration into VF in structurally and genetically normal hearts.

Our experiments identify a steeper electrical restitution curve as a quantitative marker of electrical instability in VA originating from PM. The ratio between repolarization time (RT) and cycle length (CL) identifies electrical instability prior to degeneration into VA potentially resulting in sudden death. These observations contribute to the mechanistic understanding of sudden cardiac death and may be useful in the development of new preventive therapies.

## Methods

### Study design

Ventricular arrhythmia induction and combined endo- and epicardial mapping was performed in 12 female domestic sheep (1–3 years, 37–60 kg). All animals had achieved reproductive age, ensuring that differences in hormonal maturity did not affect cardiac repolarization. One

further animal was excluded due to corrupted electrocardiogram (ECG) recordings, one did not survive until induction of VA, and a third animal was haemodynamically unstable under VA, had to receive catecholamines, and was excluded. For PM characterization, staining of Purkinje fibres ( $n = 2$ ) was performed (Figure 1).

### Anaesthesia and monitoring during electrophysiological studies

Animals were in the fasting state for 24 h before the experiment. Anaesthesia was induced by xylazine injection (i.m., 0.2 mg/kg BayerDVM, Shawnee Mission, KS, USA) and subsequent propofol infusion (i.v., 0.4 mg/kg, B. Braun, Melsungen, Germany). Anaesthesia was maintained with fentanyl as a continuous i.v. drip (0.25–2.0 mg/h, Janssen-Cilag, Neuss, Germany) in combination with 1.5% isoflurane (Abbvie, North Chicago, IL, USA). Animals were intubated and mechanically ventilated (Fabiun, Drägerwerk, Lübeck, Germany). SpO<sub>2</sub> was monitored continuously and the temperature was maintained at 36–38°C by a heated surgical blanket. Heparin was administered hourly at 2500 IU. Blood gas analysis was performed at least every hour and ventilation parameters were adjusted accordingly. General anaesthesia and monitoring were maintained during the duration of the experiment. All VA degenerated into VF while animals were under analgesic shielding and no additional agents were used for euthanasia.

### Instrumentation

A 6 Fr sheath (St Jude, Plymouth, MA, USA) was inserted into the left femoral artery for invasive blood pressure monitoring, for the administration of fluid and fentanyl, two 8 Fr sheaths (St Jude) were inserted into both femoral veins. An 8.5 Fr sheath was inserted into the right femoral artery for placement of the mapping catheter (Orion, Boston Scientific, Marlborough, MA, USA) via retrograde trans-aortic access. Left-sided thoracotomy was performed by partial removal of the third to the sixth rib.

### Induction of ventricular arrhythmia

Aconitine (Sigma Aldrich, St Louis, MO, USA) stock solution (3 µg/mL) was prepared in 50 mL distilled water, and one to two drops of 4 M HCl were added for solubility. Aliquots were stored at –20°C and thawed on ice 3–4 h before injection.<sup>16</sup> Aconitine was injected into anterior PM under echocardiographic guidance (Logic P6, GE Healthcare, Tokyo, Japan) by a Hamilton syringe (500 µL, Sigma Aldrich) with a 27 G cannula (Figure 1B and C). Strict care was taken to avoid the contact of aconitine with the epicardium. Multiple VAs were induced in 12 animals. The median injection dose was 0.06 µg [inter-quartile range (IQR) 0.06–0.15]. Aconitine was given in titrated doses to induce stable monomorphic VA and finally VF.

### High-resolution mapping

Endocardial electroanatomical mapping (Rhythmia 3D-mapping System, Boston Scientific, Cambridge, MA, USA) was performed by a 64-electrode basket catheter (8.5 Fr, Orion, Boston Scientific, Marlborough, MA, USA) during sinus rhythm (SR) and VA. Beat acceptance criteria were 12-lead ECG morphology match and time stability in relation to a reference electrogram of a surface lead. Mapping criteria CL and respiratory stability were deactivated due to the focal origin of VA and thoracotomy.

### Epicardial mapping

For epicardial mapping, a custom-made 104-electrode sock (electrode size 0.8 mm, electrode spacing 7–10 mm) was placed on the ventricular epicardium (Figure 1E), and local unipolar signals were recorded

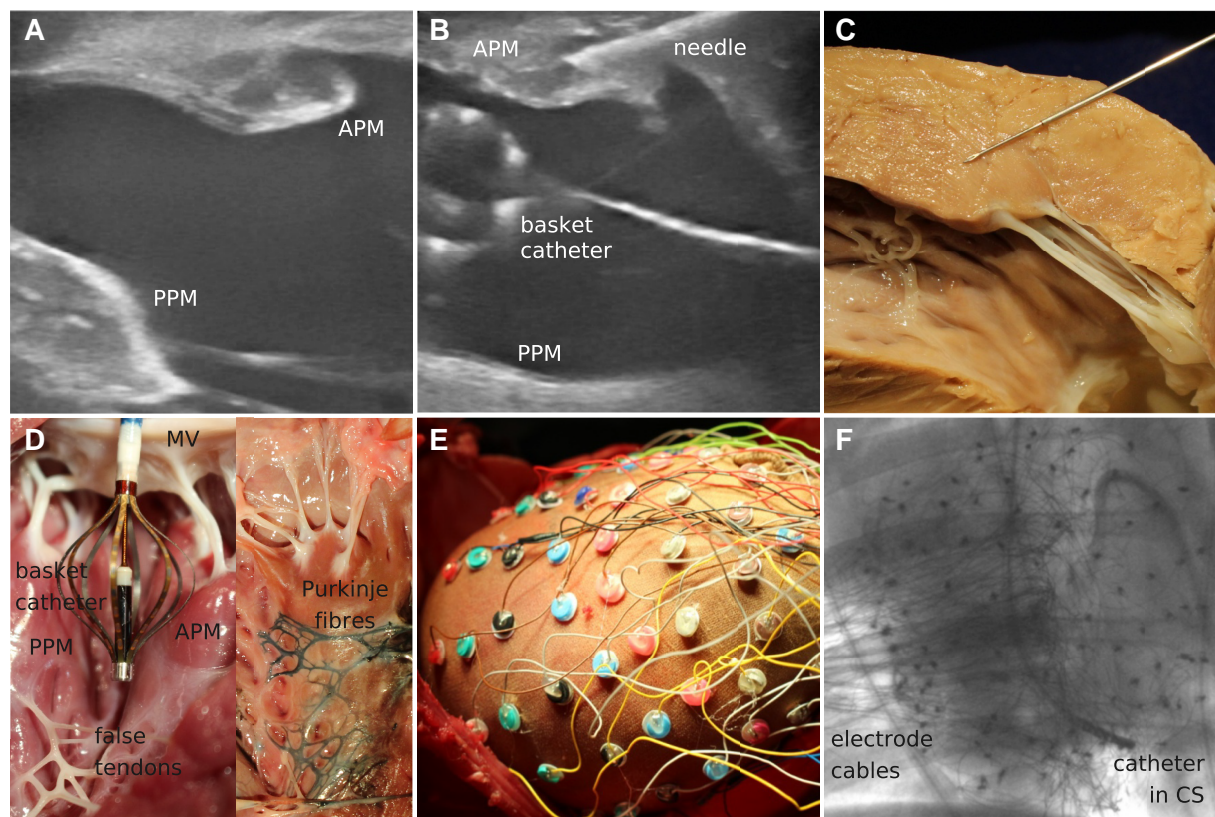


**Figure 1** Experimental set-up for endocardial and epicardial mapping of VA from PM in ovine heart. (A) Echocardiography of anterior PM (APM) and posterior PM (PPM) of the left ventricle. (B) Echocardiography during application of aconitine via injection needle. Note the multi-spline basket catheter positioned via retrograde access. (C) Left ventricular (LV) wall after formalin fixation, longitudinal dissection on level of anterior PM, correct needle position for injection of aconitine. (D) Position of the basket catheter in the left ventricle between APM and PPM, mitral valve (MV). Note the false tendons connecting LV apex to the PMs. Right: anterior PM with Purkinje fibres (Indian ink-staining). (E) Epicardial electrode sock *in situ*. (F) Fluoroscopic view of the heart in anterior–posterior projection with electrode sock on the epicardium and steerable catheter in coronary sinus (CS). APM, anterior papillary muscle; CS, coronary sinus; PPM, posterior papillary muscle.

(ME128-FAI-MPA-System, Multi-Channel Systems, Reutlingen, Germany) at a sampling rate of 20 kHz. Signals were bandstop-filtered (cut-off 200 Hz, bandstop resonator: 50 Hz,  $Q$ -factor 2.0) using MC Rack, Version 4.6.2, 2015, Multichannel System. For postprocedural analysis, data were imported into a dedicated software (EPAS<sup>20</sup>), bandpass-filtered (lower 3 Hz, upper 50 Hz) using third-order Butterworth filter. For epicardial ventricular stimulation, sock electrodes 1C and 1D (located on the posterior interventricular part of the epicardium) were connected to a stimulus generator (UHS 20, Biotronik, Berlin, Germany).

### Analysis of local activation time, repolarization time, and activation recovery interval

Intervals were defined as local activation time (LAT), RT, and ARI. Local activation time was determined as the time from reference to maximum  $dV/dt$  of the depolarization wave enabling consistent mapping of the earliest region (see [Supplementary material online, Figure S1](#)). Repolarization time was measured as the interval from reference to the maximum  $dV/dt$  of the repolarization wave. Activation recovery interval was calculated as  $RT - LAT$  as the surrogate parameter for action potential duration according to the established method<sup>9</sup> ([Figure 3C](#)). Diastolic interval is defined as  $ARI - CL$ .

### Staining of Purkinje fibres

Hearts were frozen at  $-20^{\circ}\text{C}$  for at least 12 h. After thawing, Indian Ink (VWR International, Leuven Belgium, 5% in PBS) was injected by a 30 G needle in Purkinje fibres of PM. The needle was inserted into delicate false tendons ([Figure 1D](#)) leading to the spread of Indian Ink into the Purkinje network.

### Statistics

Continuous variables are reported as medians due to the non-normality of distribution. Dispersion is reported as IQR. Parameters from unipolar electrograms consisting of a data set of 25 027 individual measurements were computed in EPAS and analysed in R 4.0.<sup>21</sup> Non-base R packages used were lme4, ggplot2, nls2, Deriv, pbapply, ggbeeswarm, ggsci, rgl, and pROC.

For pairwise comparisons, Welch's test was used for normally distributed data and Mann–Whitney  $U$  test for non-parametric data (unpaired) or Wilcoxon's test for paired, and Kruskal–Wallis test was used for global tests prior to pairwise comparisons.

### Study approval

The study protocol was approved by the local authorities of Hamburg for animal research and conforms to the Guide for the Care and Use

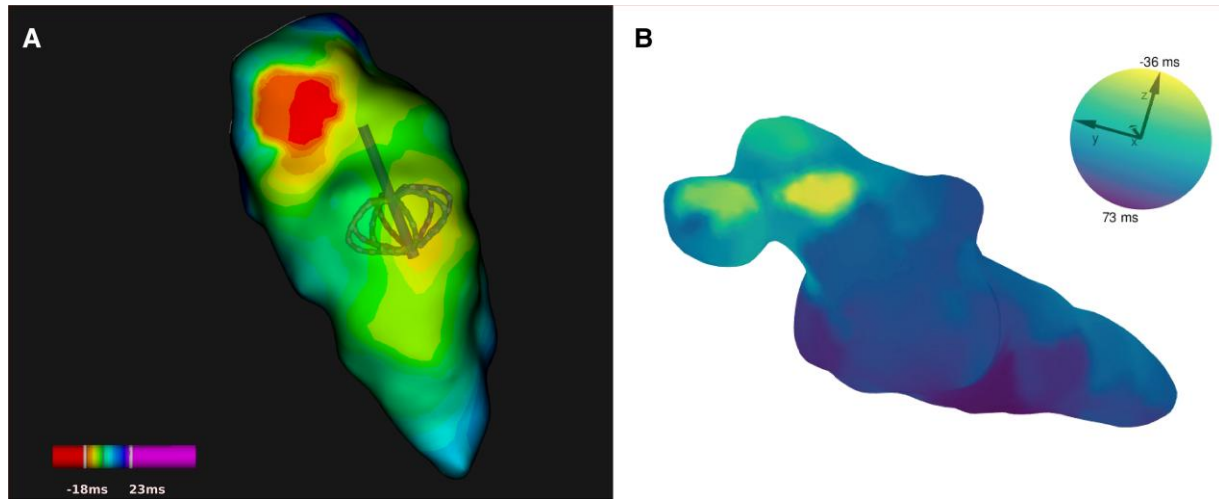


**Figure 2** Endocardial activation mapping of VA: stable VA with earliest activation at injection site in PM and faster propagation in basal direction. (A and B) Endocardial activation map of focal VA during stable VA (sequential acquisition including multiple beats) after injection of aconitine into the anterior PM, earliest activation in anterior-basal segment, by high-density mapping, legend denotes the orientation of space coordinates from mapping system and activation time colourcode (ms) (A) as represented in clinical high-density mapping, basket catheter in left ventricle (B); 3D reconstruction pseudocolour indicates LAT; see [Supplementary material online, Movie](#) for full 3D representation.

of Laboratory Animals, 8th edition, National Academy Press, updated in 2011 by the US National Research Council.

## Results

### Ventricular arrhythmia model: induction of stable ventricular arrhythmia

Focal VAs were induced in female domestic sheep ( $n=15$ ) by 71 aconitine injections into the anterior PM during endocardial and epicardial mapping under general anaesthesia after thoracotomy. Ventricular arrhythmia induction was successful in 14 animals by repeated injection of aconitine under echocardiographic control (Figure 1A and B). Cumulative individual doses are shown in [Supplementary material online, Table S1](#). Multiple VA could be induced in 12 animals for which data were included for analysis. With the exception of the last VA within each experiment, which did degenerate into VF in all experiments, VAs were self-limiting and no electrical cardioversion was performed.

### Electrocardiogram and ventricular arrhythmia characteristics

Baseline ECG in SR showed the following intervals: PR 130 ms (IQR 124–140), QRS 64 ms (IQR 56–64), QT 336 ms (IQR 332–361),  $T_{\text{peak}} - T_{\text{end}}$  56 ms (IQR 44–64). A total of 65 monomorphic sustained VA were induced and sustained in the median for 193.0 s (IQR 99.0–329.0, see [Supplementary material online, Figure S1](#)). Sustained VA occurred after median 373.0 s (IQR 311.2–515.0) following aconitine injection. Activation mapping was performed via epicardial electrode sock as well as endocardially by a 64-electrode basket catheter.

### Staining of Purkinje fibres

Purkinje fibres were stained on the endocardial surface of sheep PM (Figure 1D) revealing a dense network of Purkinje fibres and highlighting the arrhythmogenic potential of the PM and proximity of the injection site to Purkinje fibres.

### Endocardial mapping of aconitine-induced ventricular arrhythmia

During SR, a total of 29 681 mapping points were acquired including 6544 beats in 7 maps during the median mapping time of 1008.0 s (IQR 654.0–1290.0). Voltage mapping during SR showed normal endocardial voltage indicating structurally normal ventricular myocardium. A total of 186 003 mapping points were acquired via basket catheter in 44 endocardial maps during VA including 18 439 heartbeats during mapping time of median 153.0 s (IQR 104.5–286.0). The earliest activation was located at the injection site (Figure 2A and B and [Supplementary material online, Movie](#)).

### Epicardial mapping of aconitine-induced ventricular arrhythmia

A custom-made 104-electrode sock was positioned epicardially recording unipolar electrograms. Local activation time, RT, and ARI were obtained on the complete epicardial surface (Figure 3). Each electrogram was manually re-annotated for LAT and RT by a trained physician electrophysiologist for all electrodes. A total of 84 heartbeats from 14 animals were analysed for SR and ventricular pacing defined as non-VA and 135 heartbeats from 12 animals were analysed during 65 episodes of VA.

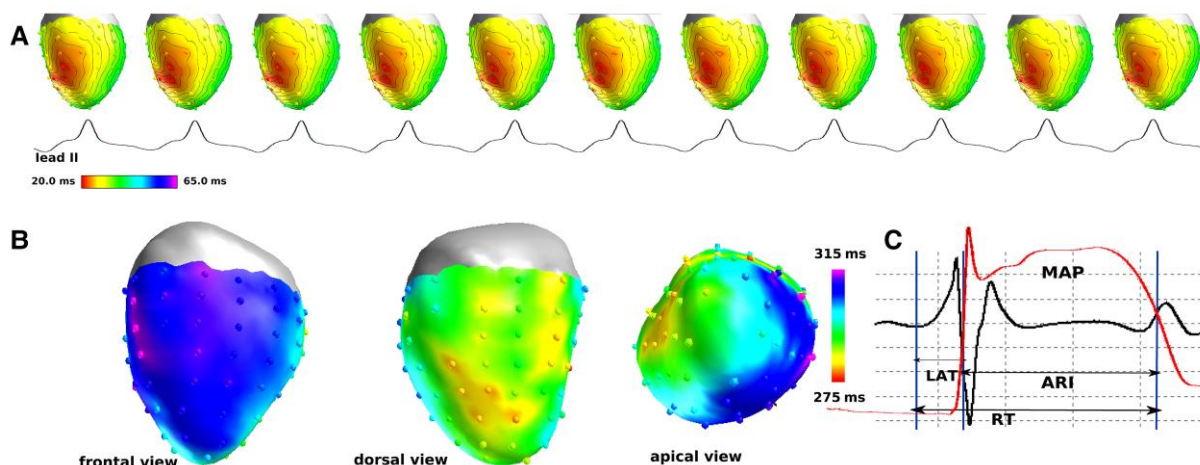


**Figure 3** Epicardial mapping of (A) LAT and (B) ARI. (A) Epicardial maps of sequential beats during ventricular tachycardia show consistent activation pattern of earliest area (global single-beat mapping). (B) Pseudocolour visualization of epicardial ARI during single beat. Epicardial maps represent ARI in frontal, dorsal, and apical projection. One exemplary unipolar signal from a single sock electrode demonstrates determination of ARI as the LAT subtracted from the repolarization time (RT). (C) ARI correlates to the monophasic action potential (MAP)<sup>6</sup> illustrated by the exemplary overlay of the MAP signal on the unipolar electrogram. ARI, activation recovery interval; LAT, local activation time; MAP, monophasic action potential; RT, repolarization time.

### Rate-dependency of repolarization time and activation recovery interval: steeper restitution curve during ventricular arrhythmia

Activation recovery interval is known to be heart rate-dependent<sup>10,11</sup> as it is influenced by the preceding DI. A known sign of electrical instability is a steep electrical restitution relation where small changes of DI lead to pronounced changes of ARI.<sup>16</sup> Electrical restitution curves were computed for ARI in relation to DI during RV pacing or SR (non-VA) and ARI during ventricular tachycardia or PVC (VA), respectively. In VA, model characteristics result in a curve for which, in all points left of its vertex, the slope was higher than in non-VA. We here exemplarily show a tangent indicating a curve slope at the arbitrary position of  $\frac{1}{2}$  of the model's horizontal limit ( $z/2$ ). The slope at  $z/2$  was 0.46 for non-VA rhythms and 1.45 for VA (Figure 4A). During VA, a given change of DI is associated with a higher change of ARI than in non-VA. A steep curve with the slope  $>1$  is considered a sign of electrical instability.<sup>16,17</sup>

### Increased repolarization time relative to cycle length in degenerating ventricular arrhythmia

To distinguish degenerating VA from self-limiting VA, we investigated the recorded parameters with respect to their potential to detect subsequent degeneration into VF: ARI, RT, DI, and CL as well as derived indices: the ratios of ARI/DI and RT/DI. Since ARI, DI, and RT are dependent on CL, we furthermore normalized the intervals by division by CL. To evaluate these parameters' potential to identify subsequent degeneration, we determined receiver operator

characteristics (ROC) which comprise the sensitivity and specificity of a given parameter to identify VA which degenerated to VF.

We here consider parameters with area under the curve (AUC) of ROC above 0.8 to combine high sensitivity and specificity for degeneration to VF. Notably, CL showed the highest AUC (0.93). Similarly, both ARI (AUC 0.9) and DI (0.9) and RT (0.88) provide a high capability for detection of degenerating VA in our model (see [Supplementary material online, Figure S3](#)). The range of values the parameters ARI, DI, and RT can exhibit is restricted by CL. After normalization to CL, only RT (RT/CL) retained a high value of AUC (0.86). For both ARI and DI normalized to CL, AUC decreased to 0.7, i.e. nearing 0.5 which indicates random association.

We computed ROC curves for additional derived parameters and composite indices based on ARI, DI, RT, and CL. The ROC AUC above 0.8 is represented in [Supplementary material online, Figures S2 and S3](#). High AUC was also found for the ratio of RT and DI (AUC 0.82, [Supplementary material online, Figure S3](#)). Repolarization time normalized to CL (RT/CL AUC 0.86, [Supplementary material online, Figure S3](#)) was significantly higher in VA which subsequently degenerated into VF compared with self-limiting VA: the median for RT/CL was 0.89 (IQR 0.8–0.95), i.e. repolarization required 89% of total CL, whereas in self-limiting VA, the median RT/CL was 0.66 (IQR 0.59–0.74) and in non-VA beats 0.52 (IQR 0.42–0.6; [Figure 5](#)).

The other two parameters with ROC AUC above 0.8 were the ratios of ARI/RT and RT/DI. The ARI/RT values were significantly higher in non-VA (median 0.85, IQR 0.81–0.89) than in self-limiting VA (median 0.83, IQR 0.79–0.87, not degenerating, [Supplementary material online, Figure S4A](#)) while both were significantly lower than in degenerating VA (median 0.69, IQR 0.63–0.78, [Supplementary material online, Figure S4A](#)), but ARI/RT ranges of non-VA and self-limiting VA were largely overlapping. In contrast,

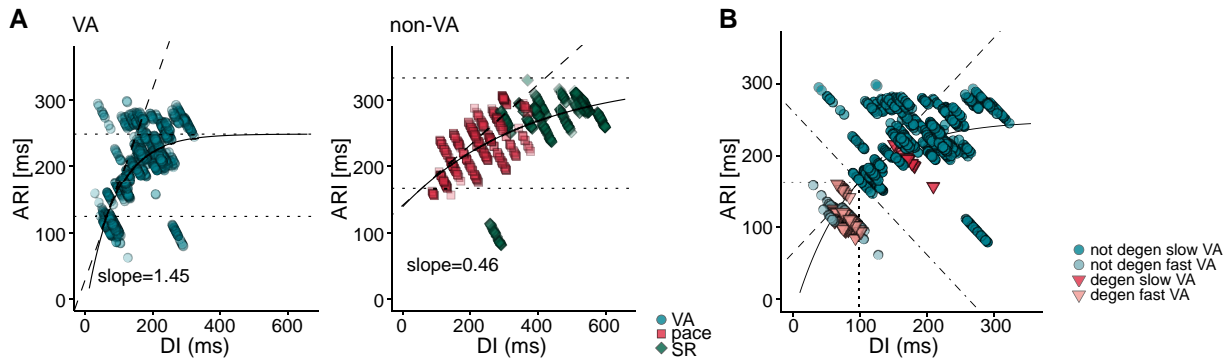


**Figure 4** Steeper electrical restitution curve for short ARI during VA (12 animals) compared with non-VA including ventricular pacing and SR (14 animals). (A) ARI in relation to DI, monoexponential model  $f(x) = z - ae^{-x/b}$ , where  $x = \text{DI}$  and ARI is a function of  $x$ . Constants of the fitted model  $a = 271.9$  ( $P = 1.8^{-51}$ ),  $b = 85.8$  ( $P = 4.8^{-21}$ ),  $z = 248.9$  ( $P = 5.8^{-280}$ ) for VA (including 135 heart beats) and for non-VA  $a = 194.7$  ( $P = 2.1^{-56}$ ),  $b = 364.8$  ( $P = 5.5^{-05}$ ),  $z = 333.9$  ( $P = 1.2^{-55}$ ), 84 heart beats. Monoexponential curves have a horizontal asymptote at  $z$  (upper dotted line) and a vertical asymptote dependent on  $a$ . A tangent is positioned at  $z/2$ , slope computed as  $f'(x) = \frac{a}{b} \cdot e^{x/b}$  at the specified point and was 1.45 for VA (left) and 0.46 for non-VA (right). (B) Normal vector at the vertex of the curve (slope of tangent = 1) was used to classify VA as fast or slow VA. Fifteen of 17 (88%) of degenerating VA and 11 of 118 (9.3%) non-degenerating VA were located below the normal vector. Individual data points represent the median ARI and DI for a beat's median interval for each of the nine anatomical regions (left anterior basal, right anterior basal, left posterior basal, right posterior basal, left anterior mid, right anterior mid, left posterior mid, right posterior mid, apical). DI, diastolic interval.

RT/DI was different with largely non-overlapping ranges in all pairwise comparisons (Supplementary material online, Figure S4B) between degenerating VA (median 2.17, IQR 1.87–2.64), stable self-limiting VA (median 1.45, IQR 1.19–1.84), and non-VA (median 0.95, IQR 0.66–1.2).

## Discussion

Lethal VA can potentially be distinguished from benign VA by an increase in the ratio between RT and CL (RT/CL). The restitution curve is steeper for VA than non-VA comprising SR and ventricular pacing. For our experiment, the index RT/CL identifies a functional propensity for lethal VA in structurally normal hearts.

For the experimental exploration of electrophysiological change preceding degeneration of VA, we induced sustained VA in healthy myocardium by aconitine injection *in vivo*. Employing this method, based on the work of Zipes and colleagues,<sup>19</sup> we were able to show stable focal VA originating from the injection site at the PM in endocardial high-resolution mapping and epicardial mapping via an electrode sock. We present a model in which VA can reliably be induced in the healthy myocardium *in vivo* and sufficiently long durations of VA are sustained to allow for detailed mapping of repeated VA in the same animal. Aconitine was used as an arrhythmic agent for its potent arrhythmic effects and induction of long sustained focal arrhythmia.<sup>19,22</sup> Arrhythmic mechanisms of aconitine have been explored during the last decades.<sup>23–27</sup> Electrophysiological effects are prolongation of the action potential,<sup>25</sup> and increased sodium conductivity.<sup>23</sup> The first patch-clamp experiment with aconitine showed an aconitine-induced shift of the membrane potential towards a more negative potential and proved that sodium channels have different modes of conduction.<sup>23</sup> Aconitine induces a burst mode of sodium channels.<sup>28</sup> Intracellular sodium concentration favouring NaCa

exchange increases intracellular calcium concentration and induces delayed after-depolarizations.<sup>27,29</sup> Delayed after-depolarization can cause triggered activation and, thus, induction of VA with degeneration into VF. Intracellular sodium and calcium overload are considered the main arrhythmogenic mechanisms of aconitine.<sup>27,30</sup>

We show that in VA, the relationship between ARI and DI is characterized by a steep electrical restitution curve, which indicates electrical instability during VA and is notably different from SR and ventricular pacing. The slope of the electrical restitution relation is a functional mapping parameter which correlates with VA and sudden death.<sup>31</sup> Previously, electrical restitution had been examined under different conditions in cardiac pacing,<sup>18</sup> but not during VA. In our study, the wide range of cycle lengths observed did allow for the representation of electrical restitution under VA. The finding of an increase in the restitution curve slope in VA builds on the traditional notion of a steep slope of the ARI~DI relation as a marker of electrical instability.<sup>16,18</sup> We here demonstrated that also in structurally normal hearts, abnormal restitution kinetics are detectable prior to potentially lethal VAs.

An established parameter to characterize electrical instability is the heterogeneity of repolarization.<sup>32</sup> In clinical practice, repolarization heterogeneity is of limited use, as plenty of data points are required.

A parameter to assess the malignancy of arrhythmia after single-beat registration would be of much higher value. We assessed the potential of various parameters to identify degeneration into VF and found high diagnostic capability as per ROC AUC values for ARI, DI, and RT. All three parameters are directly dependent on CL. Naturally, fast VAs are more likely to degenerate and are associated with shorter ARI and RT. When ARI and DI are normalized to CL, their diagnostic potential is diminished suggesting that the observed value as a classifier was mainly due to CL, i.e. short coupling interval. In contrast, RT retains its potential to identify degenerating VA even when normalized to CL. RT/CL can easily be measured in

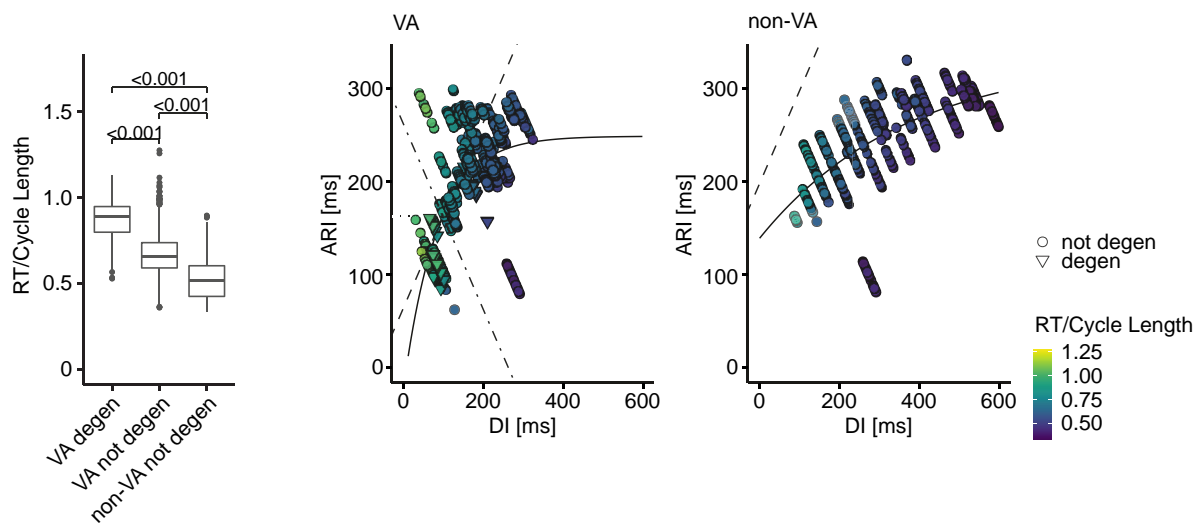


**Figure 5** Repolarization time/cycle length separates degenerating from self-limiting VA and VA from non-VA. Leftmost panel: degenerating, self-limiting VA, and non-VA beats where global Kruskal–Wallis test  $P < 0.05$ ,  $P$ -values from pairwise two-sided Wilcoxon’s test results are indicated. Centre and right panels: electrical restitution characteristics ARI vs. DI with pseudocolour overlay for predictive parameter (RT/cycle length). Solid lines indicate electrical restitution curve model  $f(x) = z - ae^{-x/b}$  where  $x = \text{DI}$  and ARI is a function of  $x$ . Dashed lines: tangent at vertex of the model; dot-dashed line: normal vector through vertex of the model separating fast from slow VA. Pseudocolour overlay indicates RT normalized to cycle length. VA, ventricular arrhythmia.

one single beat. As we observed non-overlapping ranges of RT/CL values for degenerating and self-limiting VA, theoretically a cut-off value can be defined to differentiate degenerating from self-limiting VA. However, defining such a cut-off will require extensive further research in human patients. About 1.7% of RT/CL values for non-degenerating VA were higher than the median of degenerating beats. Depending on a yet to be defined cut-off, several beats might have been classified as potentially degenerating while they were self-limiting VA in our experiment. This suggests there is a potential of the RT/CL parameter to identify single electrodynamically unstable beats probable to degenerate into VF.

Repolarization characteristics provide both high specificity and sensitivity for discrimination between self-limiting VA and degenerating VA. This observation, however, reflects the increased probability of beats with very short cycle length to degenerate into VF and it is not clear how far short cycle length itself is the decisive factor. Additional parameters which do account for cycle length dependency of repolarization, mainly RT/CL ratio, provide a similarly high capability to discern stable, self-limiting VA from VA with the propensity to degenerate into VF. Specifically, we observed repolarization comprising a median of 89% of total CL in degenerating VA, whereas in self-limiting VA, the value was 66% compared with 52% in SR. Presumably, this reflects the effect of extreme shortening of CL in accelerating VA while RT is constrained by molecular physiology, which may result in local activation by subsequent electrical impulse in incompletely repolarized tissue and eventually cause degeneration to VF. Based on the same concept, the *regional restitution instability index* consisting of a surrogate for action potential duration derived from the surface ECG divided by DI<sup>31</sup> was shown to predict VA and death in patients with ischaemic cardiomyopathy.

Correspondingly, we did observe significantly higher ARI/DI in degenerating VA compared with self-limiting VA. It is, however, not associated with a high capacity to identify degenerating VA in our study.

The observation of RT/CL as predicting degeneration of VA does neither prove causality nor does it explain the exact pathomechanism of degeneration into VF induced by aconitine. Mechanisms of aconitine have been studied in detail previously.<sup>26–30</sup> A dose-dependent effect is known.<sup>33</sup> Given that the PM *in situ* are complex anatomical structures consisting of cardiomyocytes, Purkinje fibres, insertion of tendons, and false tendons, experiments in isolated cells elucidate merely partial aspects of a complex pathomechanism underlying arrhythmia originating from PM. Effects on ion channels were not studied by the present model. Our model does, however, allow for the experimental observation *in vivo* of intra-experimental dynamics in the degeneration of stable VA into VF.

Epicardial mapping via an electrode sock in humans has so far only been performed for scientific purpose<sup>34</sup> and is not part of any clinical routine. However, the parameter RT/CL can be recorded by clinically available mapping systems, while it does warrant further validation.

Our model permits observation of arrhythmic dynamics of PM VA from endo- and epicardial surface and identified higher RT/CL in degenerating VA. This finding is relevant, as VA from PM is known as a trigger of VF.<sup>5–7</sup> In experimental studies, the PM was involved in maintaining VF.<sup>32</sup> Purkinje fibres have been identified not only as a trigger<sup>3</sup> but also as drivers of VF<sup>5</sup> and form a dense network on the PM (Figure 1D). A model of VA from PM may therefore contribute one component to a more comprehensive picture of electrophysiological pathomechanisms leading to VF.



## Limitations

The study shows an association of a higher RT/CL in degenerating VA, but does not provide mechanistic evidence that RT/CL is indeed the cause of degeneration. It merely provides one possible element in the complex pathogenesis of VF. The underlying mechanism of degeneration into VF still remains unknown.

Anaesthetic agents are possible confounders for electrophysiological parameters. In the present study, isoflurane was used which prolongs RT. However, isoflurane was consistently used in all animals so that there is a reliable baseline and equal experimental conditions did provide for internal control of the electrophysiological effects of anaesthesia. Propofol, which could be used alternatively, was not used to prevent effects on haemodynamic stability and the application of catecholamines according to need was avoided. As measurements were made in an animal model, values are not directly transferable to humans.

Taken together, the data obtained in our model indicate that (i) characteristics of the electrical restitution curves determined by pairs of corresponding DI and ARI values exhibit a notable difference between VA and non-VA with a steeper electrical restitution curve for VA and (ii) single heartbeats, represented by pairs of RT and CL values, may provide information sufficient to predict the degenerative potential of ongoing VA without the need for mapping of the complete ventricle to detect potentially arrhythmogenic substrate. A parameter which allows classification of malignancy of VA when the potential to cause life-threatening degeneration into VF is otherwise unknown and would substantially contribute to a mechanistic understanding of VF and sudden cardiac death. It may provide a diagnostic option to estimate a patient's risk for sudden cardiac death.

## Supplementary material

Supplementary material is available at *Europace* online.

## Acknowledgements

We thank Lydia Merbold for her invaluable support with the 3D mapping system for endocardial mapping (Rhythmia, Boston Scientific) and Hartwig Wieboldt for technical assistance and Aaron Diertenberger for data curation. We are very grateful for the work of the UKE animal facility, especially its animal caretakers and veterinarians. For providing relevant literature during the review process, we thank Viacheslav Nikolaev.

## Funding

The study was supported by the DZHK (German Centre for Cardiovascular Research) (FZK 81Z4710141 and FZK 81X2710180).

**Conflict of interest:** P.M. received travel grant and fellowship programme by Biotronik. C.M. received compensation for participation as consultant for Biotronik, Biosense Webster, Boston Scientific, and on speaker's bureau for Abbott, Biotronik, Boston Scientific, and Medtronic. All remaining authors have declared no conflicts of interest.

## Data availability

Raw data and code are available upon reasonable request to the corresponding author.

## References

- Ackerman M, Atkins DL, Triedman JK. Sudden cardiac death in the young. *Circulation* 2016;**133**:1006–26.
- Wellens HJJ, Schwartz PJ, Lindemans FW, Buxton AE, Goldberger JJ, Hohnloser SH et al. Risk stratification for sudden cardiac death: current status and challenges for the future. *Eur Heart J* 2014;**35**:1642–51.
- Haissaguerre M, Vignond E, Stuyvers B, Hocini M, Bernus O. Ventricular arrhythmias and the His-Purkinje system. *Nat Rev Cardiol* 2016;**13**:155–66.
- Haissaguerre M, Cheniti G, Hocini M, Sacher F, Ramirez FD, Cochet H et al. Purkinje network and myocardial substrate at the onset of human ventricular fibrillation: implications for catheter ablation. *Eur Heart J* 2022;**43**:1234–47.
- Haissaguerre M, Shah DC, Jais P, Shoda M, Kautzner J, Arentz T et al. Role of Purkinje conducting system in triggering of idiopathic ventricular fibrillation. *Lancet* 2002;**359**:677–8.
- Van Herendaal H, Zado ES, Haqqani H, Tschabrunn CM, Callans DJ, Frankel DS et al. Catheter ablation of ventricular fibrillation: importance of left ventricular outflow tract and papillary muscle triggers. *Heart Rhythm* 2014;**11**:566–73.
- Santoro F, Di Biase L, Hranitzky P, Sanchez JE, Santangeli P, Perini AP et al. Ventricular fibrillation triggered by PVCs from papillary muscles: clinical features and ablation. *J Cardiovasc Electrophysiol* 2014;**25**:1158–64.
- Ajjola OA, Yagishita D, Patel KJ, Vaseghi M, Zhou W, Yamakawa K et al. Focal myocardial infarction induces global remodeling of cardiac sympathetic innervation: neural remodeling in a spatial context. *Am J Physiol Heart Circ Physiol* 2013;**305**:H1031–40.
- Wyatt RF, Burgess MJ, Evans AK, Lux RL, Abildskov JA, Tsutsumi T. Estimation of ventricular transmembrane action potential durations and repolarization times from unipolar electrograms. *Am J Cardiol* 1981;**47**:488.
- Boyett MR, Jewell BR. Analysis of the effects of changes in rate and rhythm upon electrical activity in the heart. *Prog Biophys Mol Biol* 1980;**36**:1–52.
- Franz MR, Swerdlow CD, Liem LB, Schaefer J. Cycle length dependence of human action potential duration in vivo. Effects of single extrastimuli, sudden sustained rate acceleration and deceleration, and different steady-state frequencies. *J Clin Invest* 1988;**82**:972–9.
- Pak H-N, Oh Y-S, Liu Y-B, Wu T-J, Karagueuzian HS, Lin S-F et al. Catheter ablation of ventricular fibrillation in rabbit ventricles treated with beta-blockers. *Circulation* 2003;**108**:3149–56.
- Yue AM, Paisey JR, Robinson S, Betts TR, Roberts PR, Morgan JM. Determination of human ventricular repolarization by noncontact mapping: validation with monophasic action potential recordings. *Circulation* 2004;**110**:1343–50.
- Ng GA, Brack KE, Patel VH, Coote JH. Autonomic modulation of electrical restitution, alternans and ventricular fibrillation initiation in the isolated heart. *Cardiovasc Res* 2007;**73**:750–60.
- Yamashita S, Yoshida A, Fukuzawa K, Nakanishi T, Matsumoto A, Konishi H et al. The relationship between cardiac vulnerability and restitution properties of the ventricular activation recovery interval. *J Cardiovasc Electrophysiol* 2015;**26**:768–73.
- Garfinkel A, Kim YH, Voroshilovsky O, Qu Z, Kil JR, Lee MH et al. Preventing ventricular fibrillation by flattening cardiac restitution. *Proc Natl Acad Sci USA* 2000;**97**:6061–6.
- Nolasco JB, Dahlen RW. A graphic method for the study of alternation in cardiac action potentials. *J Appl Physiol* 1968;**25**:191–6.
- Taggart P, Sutton P, Chalabi Z, Boyett MR, Simon R, Elliott D et al. Effect of adrenergic stimulation on action potential duration restitution in humans. *Circulation* 2003;**107**:285–9.
- Inoue H, Waller BF, Zipes DP. Intracoronary ethyl alcohol or phenol injection ablates aconitine-induced ventricular tachycardia in dogs. *J Am Coll Cardiol* 1987;**10**:1342–9.
- EPLab Research Works, Warsaw, Poland. <https://eplabworks.com>. Accessed April 2022.
- R Core Team. *R: A Language and Environment for Statistical Computing*. Vienna, Austria: R Foundation for Statistical Computing, 2019. <https://www.R-project.org/>. Accessed April 2022.
- Scherf D. Studies on auricular tachycardia caused by aconitine administration. *Proc Soc Exp Biol Med* 1947;**64**:233–9.
- Peper K, Trautwein W. The effect of aconitine on the membrane current in cardiac muscle. *Pflügers Arch Gesamte Physiol Menschen Tiere* 1967;**296**:328–36.
- Dudel J, Peper K, Rüdell R, Trautwein W. The effect of tetrodotoxin on the membrane current in cardiac muscle (Purkinje fibers). *Pflügers Arch Gesamte Physiol Menschen Tiere* 1967;**295**:213–26.
- Schmidt RF. Versuche mit Aconitin zum Problem der spontanen Erregungsbildung im Herzen. *Pflügers Arch* 1960;**271**:526–36.
- Mozhaeva GN, Naumov AP, Nosyeva ED. Features of the kinetic and stationary characteristics of aconitine-modified sodium channels. *Neirofiziologiya* 1980;**12**:612–8.
- Fu M, Wu M, Wang J-F, Qiao Y-J, Wang Z. Disruption of the intracellular Ca<sup>2+</sup> homeostasis in the cardiac excitation-contraction coupling is a crucial mechanism of arrhythmic toxicity in aconitine-induced cardiomyocytes. *Biochem Biophys Res Commun* 2007;**354**:929–36.
- Nilius B, Benndorf K, Markwardt F. Modified gating behaviour of aconitine treated single sodium channels from adult cardiac myocytes. *Pflügers Arch* 1986;**407**:691–3.

29. Sawanobori T, Hirano Y, Hiraoka M. Aconitine-induced delayed afterdepolarization in frog atrium and guinea pig papillary muscles in the presence of low concentrations of  $\text{Ca}^{2+}$ . *Jpn J Physiol* 1987;**37**:59–79.
30. Zhou W, Liu H, Qiu L-Z, Yue L-X, Zhang G-J, Deng H-F et al. Cardiac efficacy and toxicity of aconitine: a new frontier for the ancient poison. *Med Res Rev* 2021;**41**: 1798–811.
31. Nicolson WB, McCann GP, Brown PD, Sandilands AJ, Stafford PJ, Schlindwein FS et al. A novel surface electrocardiogram-based marker of ventricular arrhythmia risk in patients with ischemic cardiomyopathy. *J Am Heart Assoc* 2012;**1**:e001552.
32. Pak HN, Hong SJ, Hwang GS, Lee HS, Park SW, Ahn JC et al. Spatial dispersion of action potential duration restitution kinetics is associated with induction of ventricular tachycardia/fibrillation in humans. *J Cardiovasc Electrophysiol* 2004;**15**:1357–63.
33. Tanz RD, Robbins JB, Kemple KL, Allen PA. Pharmacology of aconitine-induced automaticity of cat papillary muscle. I. Effect of dose, tension, rate and endogenous catecholamines. *J Pharmacol Exp Ther* 1973;**185**:427–37.
34. Nash MP, Bradley CP, Sutton PM, Clayton RH, Kallis P, Hayward MP et al. Whole heart action potential duration restitution properties in cardiac patients: a combined clinical and modelling study. *Exp Physiol* 2006;**91**:339–54.